

# A DEPLOYABLE SAR MEMBRANE ANTENNA MECHANICAL PROTOTYPE

M.-J. Potvin<sup>1</sup>, S. Montminy<sup>1</sup>, S. Brunel<sup>1</sup>, Y. Shen<sup>1</sup>, V. Tokateloff<sup>2</sup>, G. Akhras<sup>2</sup>

<sup>1</sup>Canadian Space Agency

6767 route de l'Aéroport, Saint-Hubert, Québec, J3Y 8Y9

Canada

<sup>2</sup>Royal Military College of Canada

Kingston, Ontario

Canada

## OVERVIEW

This work presents the current mechanical prototype of a SAR membrane antenna being tested at the Canadian Space Agency. The current concept of the C-Band membrane antenna calls for a 4 m by 10 m membrane, a wing of that antenna measuring 4 m by 5 m. The prototype measures 2 m by 3 m, which is slightly longer than a half-scale prototype of one wing. This prototype will be fully representative of the mechanical concept of the C-Band membrane antenna. The 3 horizontal layers, with the vertical layers embedded, are flattened one on top of the other for stowage. When deployed, the bottom layer and the top layer are separated by approximately 15 cm. A mechanism has been devised to tension the membranes and deploy them. The frame is made of struts and the deployment is activated from a single 6-bar linkage mechanism. The hinges are made of spring tapes, guiding devices, and a shape memory alloy. The shape memory alloy allows for a controlled deployment of the side panels of the antenna. The prototype will be tested in the fall of 2007 to assess the deployment reliability, the flatness of the frame, its stiffness, the tensioning of the membrane, the flatness of the membrane, and other properties.

## 1. INTRODUCTION

Canada has gained expertise with Synthetic Aperture Radar (SAR) antenna through Radarsat 1. Radarsat 2 is to be launched shortly, and Radarsat-C is being planned. However, these satellites all rely on rigid panels to support the dipoles forming the antenna. Added to the fact that SAR antennae are large, of the order of tens of square meters, it results in heavy antennae requiring large fairings, and therefore they are costly to launch.

Reducing the mass of the antenna and the stowage volume, if feasible, could bring important cost savings. The Canadian Space Agency, in collaboration with the Canadian private sector, has developed concepts for L-Band and C-Band membrane antennae. The C-Band antenna is made of 3 superposed horizontal layers and several small vertical layers between the second and the third horizontal layers. Work has been ongoing for several years at the Canadian Space Agency to develop all the structural elements required to deploy, tension, and maintain the flatness of a several layer membrane antenna. Moreover, a controllable lightweight hinge has been developed in collaboration with the Royal Military College of Canada.

In January 2007, after several months of studying competing ideas, a deployable frame concept was chosen. It was decided to build a near half-scale prototype in order to test all aspects of the concept: deployment of the frame, deployment of the membrane, flatness of the frame, flatness of the membrane, natural modes of the frame, tensioning of the membrane, manufacturing techniques of the membrane. The prototype is currently being integrated and tests will be carried out in the fall 2007. In January 2008, a full review of all subsystems will be carried out in order to reassess all the components and move towards a second version of the prototype.

## 2. SAR MEMBRANE CONCEPTS

In [9], a C-band membrane antenna concept developed at the Canadian Space Agency was presented. Since then, the electrical design has evolved. The C-band antenna is still made of several layers, but rather than having three horizontal layers, the concept now calls for two horizontal layers and several vertical layers has shown in FIG 1.

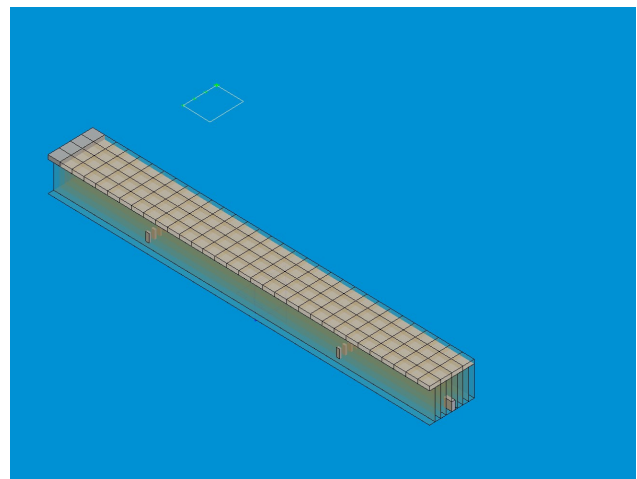


FIG 1. Subarray of a C-Band Membrane Antenna

This concept calls for the electronics to be distributed on the membrane, as shown by the little boxes grafted on the vertical layers. The two horizontal layers are separated by 1.4 cm. The vertical layers have a width of 10.5 cm. The layers should never touch each other. The two horizontal layers should out-of-plane deflections that are less than a few millimeters. This electrical design, while feasible in terms of yielding an acceptable level of power loss in the membrane at C-band, puts quite stringent conditions on

the mechanical design.

The C-band membrane antenna concept requires a 4 m by 10 m antenna, comprising two wings of 4 m by 4.5 m on each side of the bus and a panel of 4 m by 1 m above the top of the bus. Given the availability of laboratory space, it was decided to develop a prototype of one wing of the frame holding the membrane that would measure 2 m by 3 m. Such a prototype is almost a half-scale prototype of a wing, which will allow us to gain precious insight into the behaviour of the full size structure.

Due to the cost of the electrical elements, at this point, the membrane will not carry any electrical circuits. Electrical boxes will be represented by plastic boxes of the same dimensions. This first membrane prototype will allow us to perfect the manufacturing techniques, the stowage concept, the deployment sequence, and the tensioning scheme.

### 3. DEPLOYABLE FRAME

To deploy a multi-layer membrane antenna, a deployable structure is needed. Several membrane deployable structures have been proposed, most of them using inflatable booms. In [1] inflatable L-band, X-band and Ka-band spaceborne SAR prototype arrays are deployed by a rolled up inflatable mechanism. In [2], an inflatable reflector concept is developed. However, using inflatable structures requires an onboard inflation system to keep the inflated structure with a constant pressure or to rigidize the structure. This makes it more difficult to implement on a relatively small bus given the mass and volume constraints. The concept of membrane antenna deployed by foldable rigid structures has been discussed in [3]. Using foldable deployable structures to deploy a membrane antenna can provide rigid support to the membrane after its deployment and the frame can provide room to install T/R modules and other electronic parts to achieve the desired RF power distribution and beam scanning. Challenges for any of these concepts are how to deploy the folded membrane in the desired sequence without damaging the membrane and the electric parts, how to minimize the mass of the deployable structure, and how to ensure the expected stiffness of the deployed structure. In this work, we propose a structure that is deployed by two motor driven six-bar linkage mechanisms, several closed cable loops, and motion controllable hinges. The characteristics of the deployable structure are discussed. This deployable structure has the advantages of easy motion control, reliability, and low mass.

#### 3.1. Frame and Six-Bar Linkage

For a foldable deployable structure, the deployment sequence must avoid geometric interference and be done in a controlled fashion. The deployment sequence is shown in FIG 2 and 3. First, the membrane is stowed on both sides of the satellite; then, each wing deploys in the longitudinal direction, and lastly, it deploys in the two lateral directions, one after the other.

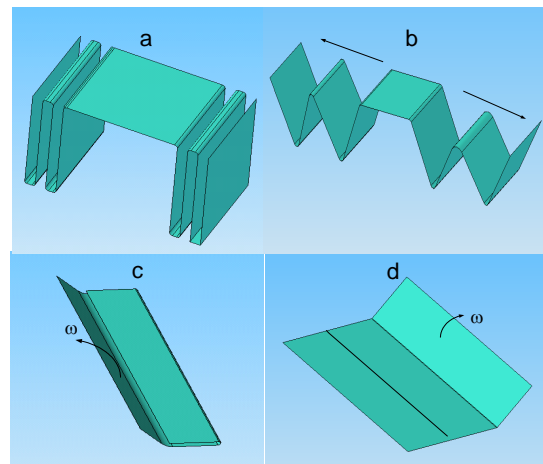


FIG 2. Membrane Deployment Sequence (a. Stowed Position b. Deployment in the Longitudinal Direction c. Deployment in One Lateral Direction d. Deployment in the Other Lateral Direction)

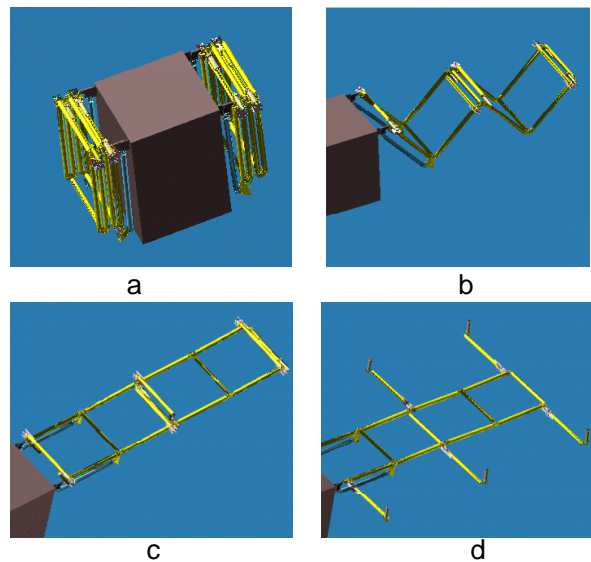


FIG 3. The Deploying Sequence of the Structure (a. Stowed State b. c. Longitudinal Deployment d. Deployment in the Lateral Direction)

To achieve this deployment sequence, we have developed a structure that can deploy the membrane in both longitudinal and lateral directions. For the longitudinal deployment, two six-bar linkage mechanisms located on both sides of the satellite, and several closed cable loops have been used. The six-bar linkage mechanism is shown in FIG 4.

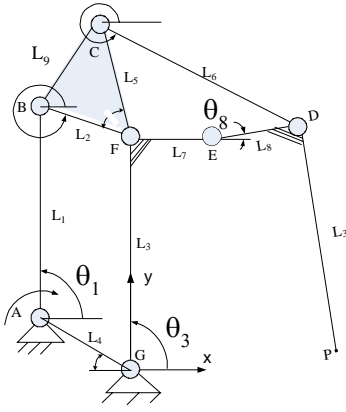


FIG 4. Six Bar-Linkage Mechanism

It is driven by a gear-head DC motor to rotate 90 degrees from its initial position to its final position, where all panels are aligned in a common plane. The motion of the frames will be highly controlled, so that dynamic loading of the structure is minimized. A closed loop control is adopted to control the motion of the motor. Since four panels need to deploy simultaneously, the closed cable loops (CCL) as shown in FIG 5 have been used.

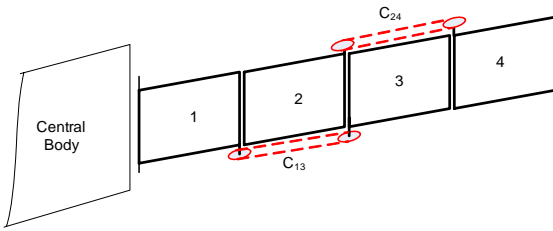


FIG 5. Closed Cable Loops on a Wing of the Antenna

A CCL is composed of two wheels whose shafts are solidly connected to two different panels respectively. The connecting cable or chain can ensure the two wheels rotate simultaneously.

As shown in FIG 4, the six bar linkage mechanism is composed of two loops A-B-F-G-A and F-C-D-E-F. The governing equations for the position constraints are

$$(1) \begin{cases} L_1 e^{\theta_1 j} + L_2 e^{\theta_2 j} = L_4 e^{-\beta j} + L_3 e^{\theta_3 j} \\ L_5 e^{-(\pi+\gamma-\theta_2)j} + L_6 e^{\theta_6 j} = L_7 e^{(\theta_3-\pi/2)j} + L_8 e^{\theta_8 j} \end{cases}$$

The lengths of the linkages can be determined based on the requirement of

$$(2) F = (\theta_8 - \pi/2)^2 \quad \text{when } \theta_3 = 0$$

The solution is obtained by using the Optimization Toolbox in MATLAB with the aim to minimize the value of F in Equation 2 with the constraint conditions of Equations 1. The dimensions of the six bar linkage mechanism are listed in TAB 1.

L <sub>1</sub>	L <sub>2</sub>	L <sub>3</sub>	L <sub>4</sub>	L <sub>5</sub>
773.4	86.19	775	95.0	135.4
8			4	6
L <sub>6</sub>	L <sub>7</sub>	L <sub>8</sub>	L <sub>BC</sub>	
135.4	30.0	30.0	89.9	
6		0	3	

TAB 1. Parameters of the Six Bar Linkage Mechanism

Assuming the driving motion on L1 is  $\theta_1 = 30t$  deg, we obtain the motion of the mechanism with the numerical simulation software ADAMS, as shown in FIG 6 and 7.

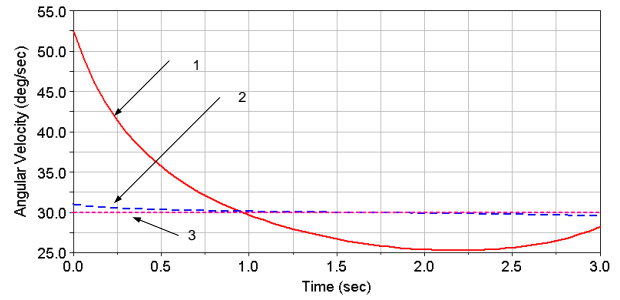


FIG 6. The Angular Velocity of the Frame When  $\theta_1 = 30t$  deg (1-DP, 2-FG, 3-AB)

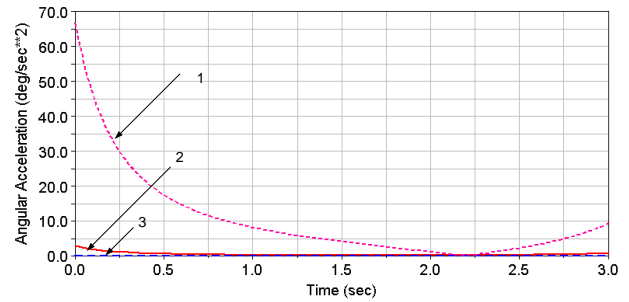


FIG 7. The Angular Velocity of the Frame When  $\theta_1 = 30t$  deg (1-DP, 2-FG, 3-AB)

From FIG 6 and 7, we find the angular velocity and angular acceleration of Linkages AB and FG are very close, but Linkage DP has a larger initial angular velocity and angular acceleration compared to AB and FG. Therefore, to obtain a smooth deployment, the drive motion  $\theta_1(t)$  needs to be carefully selected. The lateral deployment of the antenna is achieved by deploying several lateral arms which are driven by motion controllable hinges attached on each arm. These hinges are discussed in the next section.

### 3.2. Controllable Hinge Design for the Lateral Deployment of the Antenna's Frame

The hinges must be able to actuate the lateral deployment of each antenna wing in a controlled manor. It should be compact, space qualified, and lightweight. Many hinge candidates, spring and motor driven, were compared [4] before adopting the current design. Based on an earlier concept of the Tape-spring Rolamite Hinge [5], a hinge

has been designed to break the lateral deployment motion intermittently and to 'self-latch' the antenna frame into a final stiff and straight configuration. The modified hinge design, shown in FIG 8, is composed of two tape-springs, two motion guide wheels with pins, a motion control mechanism and a Shape Memory Alloy (SMA) actuator.

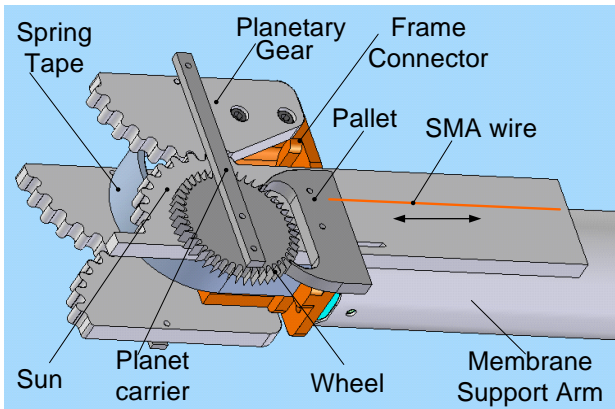


FIG 8. Modified Tape-Spring Hinge Design

Tape-springs are longitudinally curved strips of steel, comparable to carpenter tape. They are used in this project to actuate the unfolding of the hinge. When used in the above configuration, the tape-springs can release their internally stored elastic energy as they unfold to become self-locking devices that remain stiff and geometrically precise once deployed. This motion can be violent, so a deployment control mechanism is necessary to reduce the system's output inertia.

The deployment control mechanism was inspired by a traditional clock escapement mechanism (Graham pallet and wheel [6,7]), such that the one-degree of freedom hinge could deploy as the hands of a clock would unwind. Moreover, instead of using a more traditional rotary motor approach to actuate the escapement, an SMA wire is used to control the unwinding speed of the mechanism. The escapement mechanism is meant to break the hinge's deployment by allowing the tape-spring's stored elastic power to be released intermittently. The combination of the twin tape-springs and the SMA-powered escapement greatly reduces the complexity of the setup without sacrificing the hinge's low weight and volume, robustness, and electronic simplicity for similar power requirements.

The testing of the hinge was completed in two phases: first, the study of the tape-spring thicknesses to determine the moment created with respect to the hinge's deployment angle, and second, the overall functionality of the hinge with the SMA and Graham escapement mechanism. The experimental setup details can be found in [4].

The moment-rotation relationships of three different tape-spring thicknesses were measured: 0.127mm, 0.152mm and 0.178mm (0.005", 0.006" and 0.007" respectively), and are shown in FIG 9.

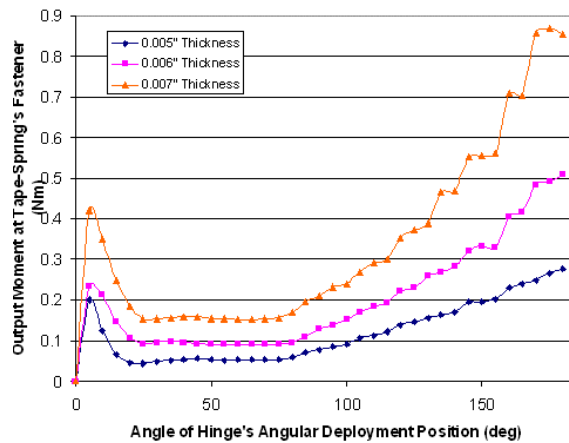


FIG 9. Experimental Results of the Moment-Rotation Behaviour During the Deployment of the Tape-Spring Hinge

The hinge was folded to 180 degrees and then gradually released to its self-locking 0-degree deployed position. The deployment's pattern is very similar to that found in [8]. An initial kick-off higher moment begins the unfolding of the hinge; the moment then diminishes and stabilizes, followed by a jump in the output moment during the tape's unbuckling and snapping into place.

Many deployment runs were conducted for the functionality testing of the hinge with the SMA-controlled escapement. Though some problems were encountered, it was possible for the hinge to deploy completely and independently. The main challenges were mechanical play, excessive friction between the wheel teeth and pallet, and SMA-crimp slipping. Future prototypes will be modified to increase the reliability. Tape-spring hinges combined with an SMA-powered escapement present an interesting lightweight and compact option for a controlled lateral deployment of the SAR antenna frame. The SMA parameters (SMA dimensions, input current) still require optimization. Thermal analysis should be carried out to ensure the system's performance in the rigorous space environment.

## 4. THE TENSIONING SYSTEM

Once the frame is deployed, the layered membrane needs to be tensioned. The tensioning bars, described below, will separate the layers and apply tension. The cable system will relay this tension to the membrane. Tensioning plates will serve as attachment points between the cables and the tensioning bars.

### 4.1. Tensioning Bars

The tensioning bars have two main purposes. Firstly, they are used to separate the three membrane layers from each other, once the lateral deployment is completed. Then, they are used to apply tension on the membrane layers at the end of the deployment sequence. In fact, in order to prevent any damage on the membrane during the deployment, this device allows the tension in the entire frame to be released in the stowed configuration.

The tensioning bar is a mechanism that pivots around a shaft in order to give the membrane assembly a 3D shape. This mechanism also contains a spring loaded rotary drum capable to be released and thus apply the tension necessary to achieve the flatness requirement in the membrane. The deployable antenna design contains six tensioning bars located at the tip of each lateral bar. FIG 10 shows the way the tensioning bars are arranged on the deployable frame.

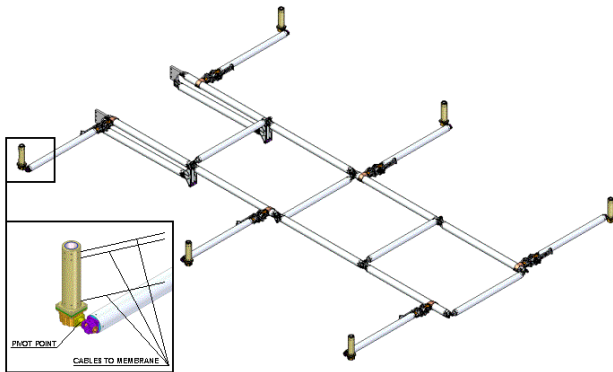


FIG 10. Tensioning Bar Mechanism Arrangement

Each layer of the membrane is bordered by a cable, which is used to tension the membrane. The extremities of the cables are attached, through a tensioning plate described later, to the pre-loaded drums located inside the tensioning bars. The pre-loading is done using a ratchet/pawl system and the energy is stored into a constant force spring. The actual version of the mechanism can be cranked via a screw driver recess located at one end of the tensioning bar mechanism.

The mechanism is released by "pushing" a mechanical lever (pawl) that disengages the ratchet wheel that is connected to the constant force spring. Once released, the drum rotates up to 2 turns with respect to the chassis and 5 cm of cable is then enrolled onto it in order to apply the tension. In the present version of the mechanism, the impulse necessary to release it is done manually but it is planned to be accomplished by a shape memory alloy (SMA) actuator in the next version. FIG 11 shows an exploded view of the mechanism.

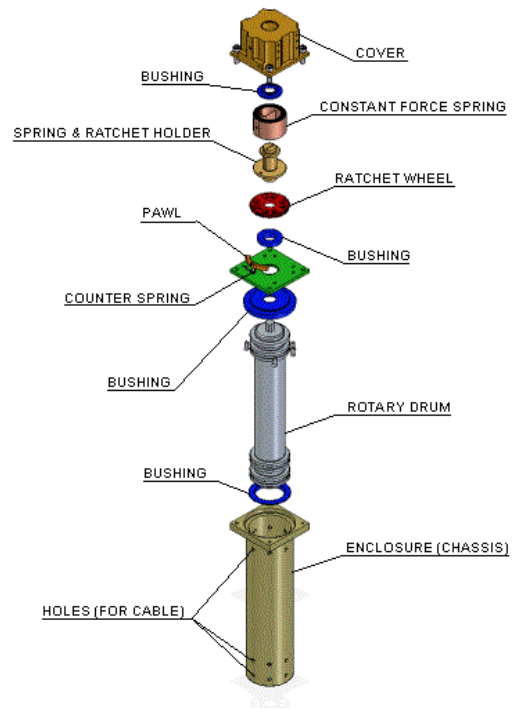


FIG 11. Exploded View of the Tensioning Bar Mechanism

The functionality of the tensioning bar mechanism was tested on a preliminary version. Most of the parts comprised in this device are made of aluminum, except the springs and the ratchet wheels, which are made of stainless steel, and also the bushings, made of PTFE (Teflon®). The mass of the entire assembly is approximately 180 grams. FIG 12 shows the tensioning bar mechanism.

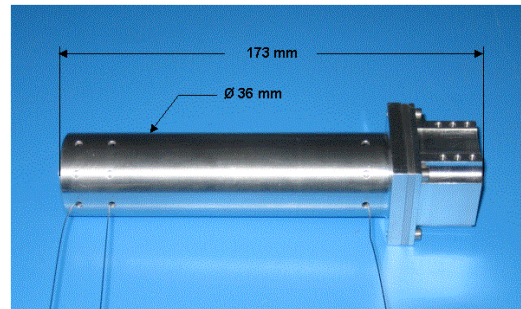


FIG 12. Tensioning Bar Mechanism Assembly

#### 4.2. Tensioning Scheme for a Nonsymmetrical Frame

Various authors have written about how to tension a membrane within a frame. A simple, yet efficient, approach uses parabolic cables, as demonstrated in FIG 13, allowing to tension a membrane with few holding points. With this approach the in-plane tension is distributed evenly. The remaining wrinkles are caused by manufacturing defects as outlined in [9].

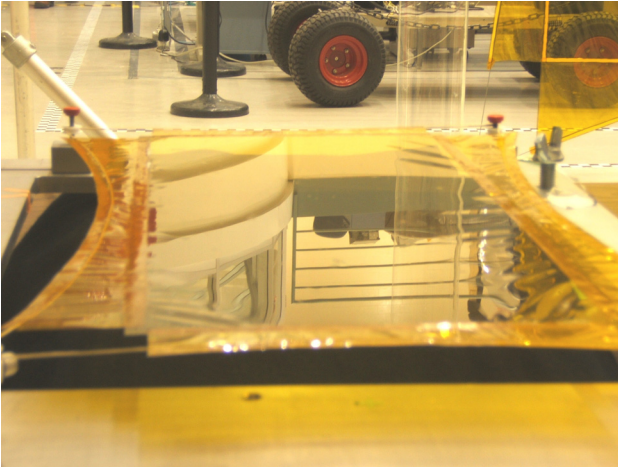


FIG 13. Membrane Tensioned with Parabolic Cables

The equations defining the parabolas and the resulting in-plane tension of the membrane are discussed in [10,11] among others. However, these schemes all assume a symmetrical frame holding the membrane. In our case, in order to provide a foldable frame as compact as possible, the holding points of the membrane are all offset with respect to one another, as shown in FIG 14.

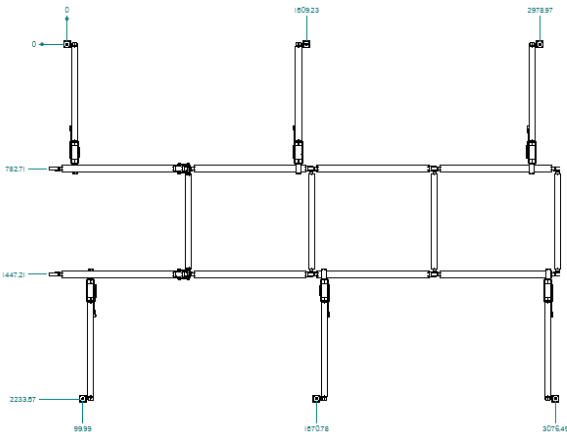


FIG 14. Deployable Frame

The design of the frame fixes a few parameters of the tensioning system. The holding points are fixed. Using the following equation taken from [12]:

$$(3) \quad T_{\max} = \frac{W \cdot L}{2} \sqrt{\frac{L^2}{16h^2} + 1}$$

the tension as the cable exits the pocket,  $T_{\max}$ , is defined with respect to  $W$ , the in-plane tension for a given thickness,  $L$ , the length of the pocket, and  $h$ , the depth of the pocket. For this prototype the in-plane tension has been fixed at  $140 \times 10^3$  Pa. Past experience has shown this value to provide enough flatness in the membrane if the manufacturing defects in the tensioning system are small. However, this level of in-plane tension does not prevent the occurrence of out-of-plane motion when the frame is excited. There would be a loss of signal when the

satellite would undergo attitude control manoeuvres. We are currently using Kapton E membrane of a thickness of  $25 \mu\text{m}$ . This leads to a value for  $W$  of:

$$(4) \quad W = 140 \times 10^3 \text{ Pa} \cdot 25 \mu\text{m} = 3.5 \text{ N/m}$$

Both the values of  $T_{\max}$  and  $h$  should be minimized:  $h$  in order to reduce the size of the frame holding the membrane, and  $T_{\max}$ , in order to reduce the load on the frame and allow for a lighter, slenderer frame. Of course, looking at Equation 3 shows that both cannot be minimized simultaneously, and therefore, iterations are required to establish a trade-off.

At both extremities, the holding points are not at the same height with respect to the membrane. A slightly modified version of Equation 3 is used in that case, also taken from [12]:

$$(5) \quad \begin{aligned} T_A &= W \cdot L_A \sqrt{1 + \frac{L_A^2}{4h_A^2}} \\ T_B &= W \cdot L_B \sqrt{1 + \frac{L_B^2}{4h_B^2}} \end{aligned}$$

where in this case,  $T_A$  and  $T_B$  are the maximum tensions as the cable exits the pocket at end A and B of the width of the membrane.  $L_A$  and  $L_B$  are the distances between the minima of the parabola and the extremities A and B of the pockets.  $h_A$  and  $h_B$  are the depths of the pocket at extremities A and B, the depth being the distance between the minima of the parabola and the height of the parabola at the extremity. The difference between  $h_A$  and  $h_B$  is set by the physical dimensions of the frame. In the case of our prototype, there is a 10 cm difference between the height of extremities A and B.

The shapes of the different parabolae will dictate the angles at which the cables exit the pockets and can be attached to the holding points of the frame. As shown in FIG 10, cables exit the tensioning bars to allow tensioning the membrane. The cables from the middle tensioning bars exit the bars directly ahead towards the membrane, whereas the cables of the corner tensioning bars exit the bars at  $45^\circ$ . If we were to attach the cables from the membrane directly onto the cables coming from the tensioning bars, the angle of the either cable would be modified. In the case of the cables coming from the pockets, this would result in a loss of tension or in an unequal tension in the membrane producing wrinkles; in the case of the cable coming out of the tensioning bar, changing the angle of the cable would lead the cable to touch the side of the tensioning bar, creating friction and reducing spring-loaded induced tension in that cable. In all cases, the system will work optimally if the cables remain at the angles they were designed for. Parts were therefore required to interface between the cables coming out of the tensioning bars and the cables coming out of the pockets around the membrane.

### 4.3. Tensioning plates

Triangular parts, such as the one shown in FIG 15, were designed to ensure all cables would keep their intended angles.

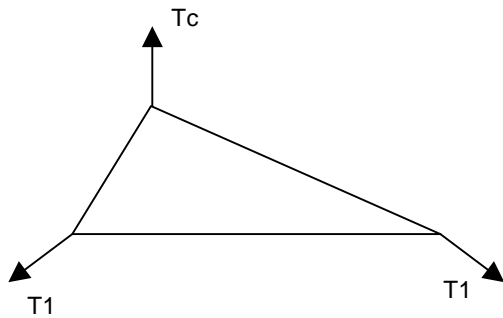


FIG 15. Tensioning Plate for the Central Tensioning Bars

FIG 15 shows the specific tensioning plate used for the central tensioning bars. Accordingly, the cable going to the tensioning bar points directly up from the triangle with a tension  $T_C$ . The other two cables come out of identical pockets, since the lateral pockets are all identical. As a result, both the tensions and the angles of these cables are the same. For the corner tensioning plates, the three cables would have different angles and tensions.

In order to avoid any modification in the angles or the tensions of the three cables, the tensioning plate must be balanced. The tensions  $T_1$  are known, as well as the angles of the three cables. The remaining unknown is the value of  $T_C$ . The equations representing the sums of the forces and the moments around one corner are written and allow to find the required value of  $T_C$  to balance the tensioning plate.

Because there are 3 different sets of tensioning plates to balance (the plates in the middle of the frame, the plates at end A of the parabolae of the extremities frame, and the plates at end B of the parabolae of the extremities of the frame), an iterative process is needed. From this, the best set of  $h_A$ ,  $h_B$ , and  $h_1$  is found to ensure low loads on the frame, equilibrium of all tensioning plates, and maximising of the antenna surface. The tension applied on each tensioning bars are derived from these calculations. With the current prototype, the tension on the two middle tensioning bars is 4 N for each layer; on the side of end A of the extremity parabolae, the tension is 11.1 N for each layer; on the side of end B of the extremity parabolae, the tension is 11.6 N for each layer. The Maple worksheet detailing the equations and the iterative process is available from the first author upon request.

## 5. FINITE ELEMENT ANALYSES OF THE FRAME

Preliminary static and modal analyses were carried out on the frame prototype representative model. The first goal is to evaluate if the frame will deform under the loading caused by the tensioning of the membrane. The second

goal is to obtain the natural frequency of the frame in order to evaluate the ability of the frame to remain steady when attitude control manoeuvres are done. These manoeuvres typically excite modes below 5 Hz.

### 5.1. Finite element model

The finite element model is representative of the prototype in terms of mass and rigidity. Each tube was represented with beam elements and each mechanism with solid and shell elements. The various parts are connected together by rigid elements. At this stage, the membranes are not represented. The current model contains 1328727 degrees of freedom. FIG 16 shows the model in the vicinity of the mechanisms.

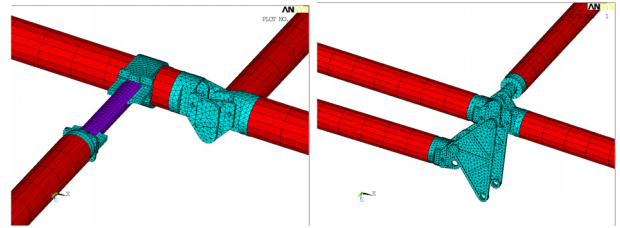


FIG 16. Finite Element Model in the Vicinity of the Mechanisms

### 5.2. Boundary Conditions

The applied boundary conditions are representative of the prototype test conditions. The six bar linkage base is embedded; gravitational acceleration is applied on the whole model and the membranes tension loads are applied. FIG 17 shows the boundary conditions.

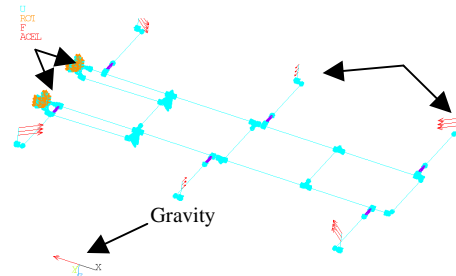


FIG 17. Boundary Conditions

### 5.3. Results

Preliminary results have been obtained for both the static analysis and the modal analysis.

#### 5.3.1. Static Analysis

The static analysis shows a maximum displacement of 13.6 mm, with a maximum flatness difference of 8.2 mm between the tops of the tensioning bars. FIG 18 shows the results of the static analysis. One can see the deformation of the frame. Given the tight flatness requirement to obtain the desired reliability for a C-band membrane antenna, these results need to be improved. The frame will need to be stiffened.

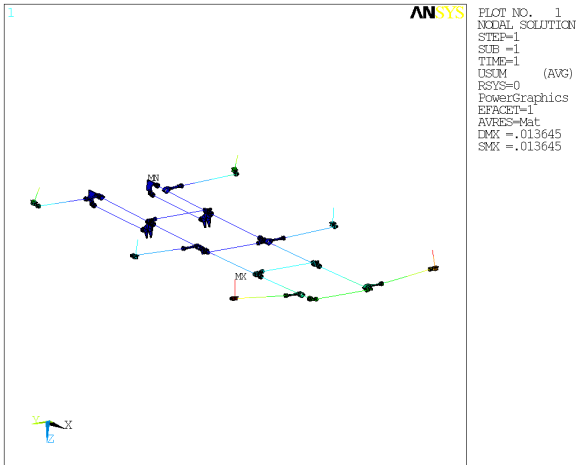


FIG 18. Static Analysis Results

### 5.3.2. Modal Analysis

The modal analysis; carried out on the statically pre-stressed model; shows a first natural frequency of the structure at 2.7 Hz. FIG 19 shows the first mode of the frame.

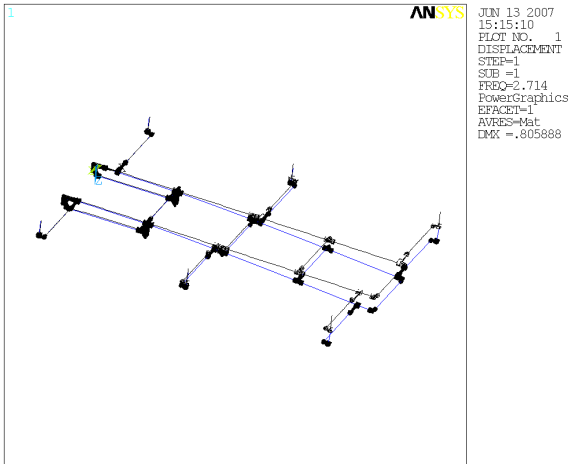


FIG 19. First Mode of the Frame

TAB 2 enumerates the first six natural frequencies:

Mode	1	2	3	4	5	6
Freq. (Hz)	2.71	5.62	6.99	12.35	12.69	14.29

TAB 2. Natural Frequencies of the Frame

To avoid any vibration during attitude control manoeuvres, the first natural frequency is usually required to be above 5 Hz. The frame should be stiffened; otherwise, loss of signal from the antenna can be expected during attitude control manoeuvres.

## 6. CURRENT PROTOTYPE

The entire deployable frame, mainly made of aluminium, was manufactured in the CSA's fabrication facility using a numerically controlled milling center and a conventional

lathe. The overall mass of the frame is around 18 kg, including all the mechanisms, except the motor-transmission system necessary to deploy the six bar linkage mechanism. The overall dimensions in the deployed configuration are approximately 3.2m x 2.3m x 0.3m, whereas the overall dimensions in the stowed configuration are 1m x 0.9m x 0.6m.

The frame is still under integration and it will be subjected to testing once fully assembled. FIG 20 shows the assembly in its current status. Note that three of the six lateral arms, as well the related hinges and tensioning legs, still need to be integrated .

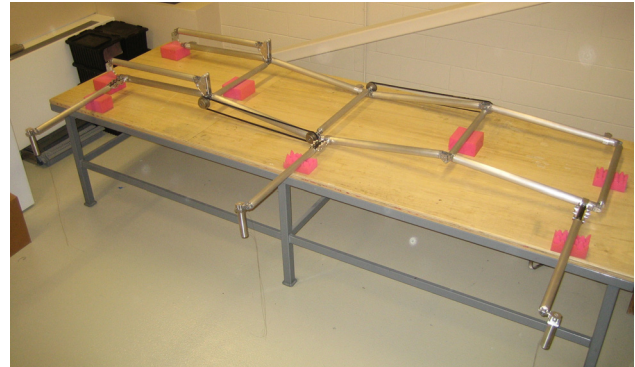


FIG 20. Antenna Frame Prototype (Deployed Configuration)

The six bar linkage mechanism was integrated and the functionality has been validated prior to going further into the integration process. FIG 21 shows both ends of the six bar linkage.



FIG 21. Prototype of the Six Bar Linkage

FIG 21 also shows one end of the timing belt/pulley system used to transfer the motion produced by the six bar linkage to the other foldable sections of the frame. A significant amount of material needs to be shaved from the pulleys in order to reduce the mass.

FIG 22 shows the deployable frame in the stowed configuration.



FIG 22. Antenna Frame Prototype (Stowed Configuration)

Once the integration of the frame is completed, the membrane and the tensioning plates will be added. Tests will include deployment tests of the frame, flatness measurements of the frame, modal tests on the frame alone, tensioning tests of the membrane, and flatness measurements of the tensioned membrane.

## 7. CONCLUSIONS AND FUTURE WORK

The Canadian Space Agency has been working for several years on the C-band membrane antennae. Lately, several techniques matured enough to envision building a near half-scale prototype. We have settled on a deployable frame, by opposition to an inflatable frame, to avoid imposing any compressor on the bus. The C-band membrane has two horizontal layers and several vertical layers with distributed electronics. Preliminary analyses show that the current design will need to be stiffened in order to achieve the required membrane flatness, which is less than 1 cm out-of-plane deflection on a complete 4 m by 10 m membrane. Testing of the prototype will occur during the fall of 2007. In January 2008, a full review of each subsystem will be carried out in order to produce a second, more performing, version of the near half-scale prototype by the spring of 2009.

## REFERENCES

- [1] Huang, J. et al, "The development of inflatable array antennas," IEEE Antennas and Propagation Magazine, Vol. 43, No.4, 2001, pp.44-50.
- [2] Thomas, G. and Veal, G., "High accurate inflatable reflectors," Report AFRPL TR84-023, May, 1984.
- [3] J. Huang, M. Lou, and E. Caro, "Super-low-mass spaceborne SAR array concepts," IEEE AP-S/URS1 Symposium, Montreal, Canada, July 1997, pp.1288-1291.
- [4] Tokateloff, V., Akhras, G., Potvin, M.-J., Montminy, S., Shen, Y., "A Controllable Hinge Mechanism for the Deployment of a SAR Satellite Antenna", CASI Aero 2007 Conference Proceedings, Toronto, April 2007.
- [5] Watt, A.M., Pellegrino, S., "Tape-Spring Rolling Hinges", Department of Engineering, University of Cambridge, Proceedings of the 36th Aerospace Mechanisms Symposium, Glenn Research Centre, May 2002.
- [6] Britten, F. J., "Britten's Watch and Clock Maker's Handbook Dictionary and Guide", Arco Publishing Company, New York, 1978.
- [7] Headrick, M. V., "Clock and Watch Escapement Mechanics", Mark Headrick's Horology Page and E-Book, 1999, <http://www.geocities.com/mvhw>, or <http://www.abbeyclock.com/escpdf.html>
- [8] Pellegrino, S., Keadze, E., Lefort, T., Watt, A. M., "Low-Cost Hinge for Deployable Structures", CUED/D-STRUCT/TR202, Astrium Contract No. 24070108, July 2002.
- [9] Colinas, J., et al. Recent developments on C-band membrane antennas for small-satellites applications, Proceedings of the 28<sup>th</sup> ESA Antenna Workshop on Space Antenna Systems and Technologies, Noordwijk, Holland, May 31-June 4, 2005.
- [10] Fang H., et al. Catenary Systems for Membrane Structures, Proceedings of the 42<sup>nd</sup> AIAA/ASME/ASCE/AHS/ASC Structures, Structural Dynamics, and Materials Conference and Exhibit, Seattle, Washington, April 16-19, 2001.
- [11] Potvin M.-J. and Montminy S. Catenary System for a Flat Membrane Antenna Supported by an Inflatable Structure, Proceedings of the ASTRO 2002 Conference, Ottawa, November 12-14, 2002.
- [12] Riley, W.F., Sturges, L.D. Engineering Mechanics, Statics, John Wiley and Sons, New York, 1993.